

# An Experimental Method for Determining Dynamic Fracture Toughness

by C. H. Popelar, C. E. Anderson, Jr. and A. Nagy

**ABSTRACT**—The boundary and loading conditions in many dynamic fracture test methods are frequently not well defined and, therefore, introduce a degree of uncertainty in the modeling of the experiment to extract the dynamic fracture resistance for a rapidly propagating crack. A new dynamic fracture test method is presented that overcomes many of these difficulties. In this test, a precracked, three-point bend specimen is loaded by a transmitter bar that is impacted by a striker bar fired from a gas gun. Different levels of energy can be imparted to the specimen by varying the speed and length of the striker to induce different crack growth rates in the material. The specimen is instrumented with a crack ladder gage, crack-opening displacement gage and strain gages to develop requisite data to determine toughness. Typical data for AISI 4340 steel specimen are presented. A simple quasi-dynamic analysis model for deducing the fracture toughness for a running crack from these data is presented, and the results are compared with independent measurements.

**KEY WORDS**—Dynamic crack growth, impact, fracture test, dynamic fracture toughness

## Introduction

An essential part of any fracture mechanics methodology for rapid crack propagation and crack arrest is the determination of the dynamic fracture toughness—the material's intrinsic resistance to crack propagation. Many different dynamic fracture tests and specimens have been used in this determination. Quasi-static loading of a specimen with a blunt starter notch has been used to create a supercritical condition to produce a rapid propagating crack as it initiates from the notch.<sup>1</sup> The energy available to drive the crack under displacement-controlled loading is limited by the elastic energy stored in the specimen prior to initiation of crack growth and is proportional to the planar area of the specimen. While this approach suffices for high strength, low toughness materials, it is inadequate for lower strength, higher toughness materials because it is virtually impossible to store sufficient elastic energy to drive the crack through the specimen. To overcome this limitation, Couque, Leung and Hudak<sup>2</sup> developed the coupled pressure bar test in which elastic energy is stored in external pull bars and transferred dynamically to the specimen.

A pendulum or drop-weight machine<sup>3</sup> was used to initiate and extend a rapidly propagating crack. A precise measurement of the load applied to the specimen was usually difficult. The interpretation and analysis of the experiment can be confounded by intermittent loss of contact between the specimen and the anvil and/or supports.

van Elst<sup>4</sup> used a gas gun to fire, at speeds of 70 m/s to 80 m/s, a steel projectile 600 mm long and 40 mm in diameter at prenotched, three-point bend specimens of line pipe steels. The projectile partially pierced the specimen and produced excessive plastic deformation at impact. A rather sophisticated analysis of the highly instrumented test was required to extract the fracture resistance.

Rittel, Maigre and Bui<sup>5</sup> used a split Hopkinson bar arrangement and a compact compression fracture specimen to measure the dynamic initiation fracture toughness. The special geometry of the specimen permitted the crack to open under impact loading of the incident bar. Because the specimen was not loaded symmetrically, a mixed mode I and mode II loading of the crack tip occurred. The authors assumed the crack-opening mode (mode I) to be dominant when deducing the initiation toughness from the measurements.

Yokoyama<sup>6</sup> used a variation of a split Hopkinson bar method to determine the dynamic fracture initiation toughness using a precracked, three-point bend specimen 100 mm long by 20 mm high by 10 mm thick. Loading was through a transmitter bar in contact with the specimen that was impacted by a high-strength steel striker bar 700 mm long and 16 mm in diameter fired from a gas gun. Strain measurements on the transmitter bar and support pressure bars were input to a finite element model of the test to determine the dynamic initiation toughness for 7075-T6 aluminum, Ti-6246 alloy and AISI 4340 steel.

A new dynamic fracture test method is presented in which an instrumented, precracked, three-point bend specimen is dynamically loaded through a transmitter bar that is struck by a striker bar fired from a gas gun. The duration and intensity of the loading pulse delivered to the transmitter bar and ultimately to the specimen is controlled by the length and speed of the striker bar. This test arrangement has several advantages over other dynamic fracture test methods. For example, high-speed video equipment and synchronization are not required, and no special preparation (e.g., polishing) of the specimen is needed. The test does require a gas gun. The initial and boundary conditions for the test are well defined. A detailed description of this test apparatus and method are given in the following sections. Typical data are presented for dynamic fracture tests conducted on AISI 4340 steel. A simple quasi-dynamic analysis is used to deduce the

C. H. Popelar is an Institute Engineer, C. E. Anderson, Jr., is Director and A. Nagy is a Staff Engineer, Southwest Research Institute, San Antonio, TX 78228-0510.

Original manuscript submitted: October 10, 1999.  
Final manuscript received: August 7, 2000.

fracture toughness for a running crack from these data, and the results are compared with independent measurements of Zehnder and Rosakis.<sup>3</sup>

### Dynamic Fracture Test Method

In the test arrangement, a fatigued, precracked, three-point bend specimen is contained within a massive steel base fixture as depicted in Fig. 1. The specimen is supported by two 25.4-mm-diameter pins made of a high-grade alloy steel and located 165.1 mm on centers. Spacer plates are used to position the specimen in the fixture. The specimen is loaded through a 254-mm-long and 25.35-mm-diameter transmitter bar by a 25.32-mm-diameter striker bar that is fired from a gas gun. Both bars are made from VASCOMAX 350 CVM, a maraging steel with a yield strength of approximately 2.3 GPa. The end of the transmitter bar in contact with the specimen is machined to produce a line load. The length of the striker bar and its speed determine, respectively, the duration and intensity of the generated loading pulse. In the tests reported herein, the length of the striker bar is 138.7 mm. While striker bar speeds up to 120 m/s can be attained with the gas gun, the maximum speed is limited to approximately 90 m/s to avoid yielding of the bars.

The supporting base fixture is bolted to the flange of a large, wide beam on which a gas gun is mounted. Figure 2 provides an overall view of the setup showing the test bench, gas gun, specimen holder and instrumentation. Figure 3 shows a closer view of the supporting fixture. The fixture is aligned so that the axes of the transmitter and striker bars are collinear. The speed of the striker bar as it exits the gun barrel was calibrated against the gas pressure in the gun. By adjusting the pressure, the striker bar's speed can be controlled. Two photodiodes are used to provide an accurate measurement of the impact speed.

### Fracture Specimen

The planar dimensions of the three-point bend specimen (see Fig. 4) are 50.8 mm by 203.2 mm, and the thickness is 24.35 mm. It contains a centrally located, through-thickness, machined notch that is approximately 16-mm deep. One face of the notch is relieved to accept an eddy current proximity gage for measuring the crack-opening displacement (COD) during the dynamic fracture event. This specimen contains side grooves that have approximately 10 percent relief on

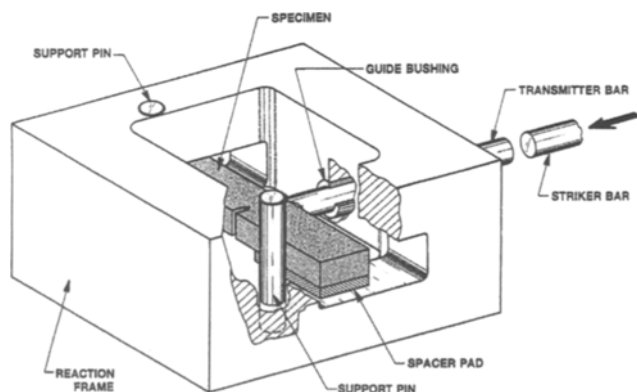


Fig. 1—Schematic of dynamic three-point bend test apparatus

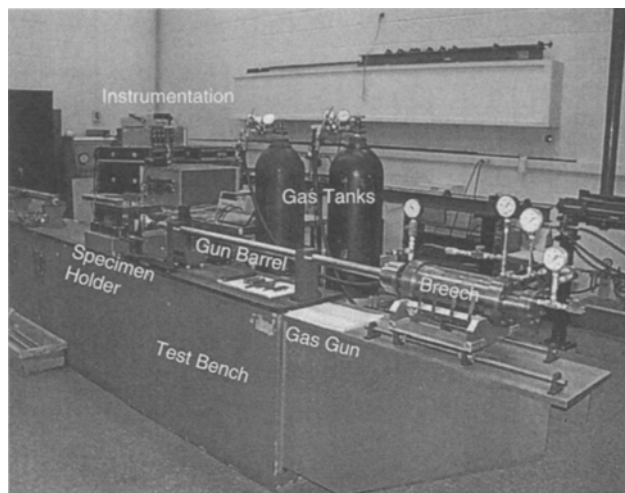


Fig. 2—Overall view of test setup showing test bench, gas gun, specimen holder and instrumentation

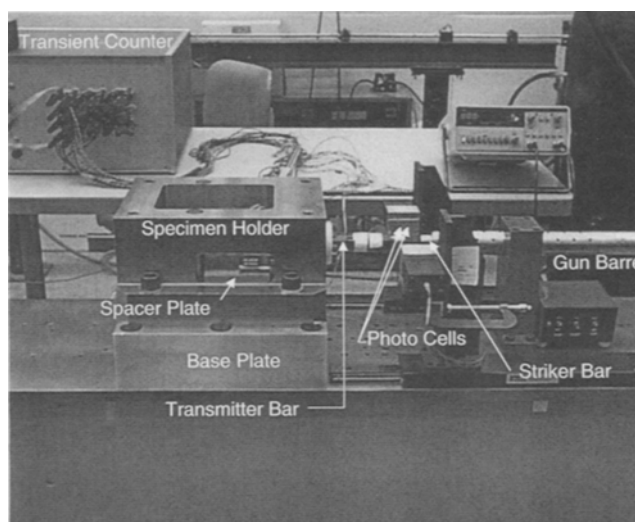


Fig. 3—Close-up view of test apparatus

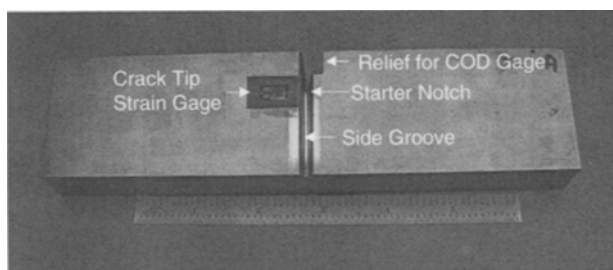


Fig. 4—Photograph of the dynamic three-point bend specimen showing the starter notch, side groove and relief for the crack-opening displacement (COD) gage

each side of the specimen to promote plane strain fracture and preclude bifurcation or curving of the crack during the test.

A sharp fatigue crack is introduced at the base of the machined notch by cyclically loading the specimen between a maximum stress intensity factor of approximately 60 percent of the plane strain fracture toughness  $K_{Ic}$  and a minimum

stress intensity factor equal to 10 percent of the maximum value (i.e.,  $R$  ratio = 0.1). The fatigued crack typically is allowed to grow 1.5 mm beyond the machine notch.

The specimen is instrumented in several ways. One strain gage is located approximately 10 mm opposite the fatigue crack tip (see Fig. 4). A KAMAN Instrument Corporation Model 2UB eddy current sensor is used with a Model KD 3210-2UB oscillator/demodulator to measure the COD. The sensor is 10.8 mm in diameter and 6.35 mm thick. This COD gage has a linear range over approximately 2.5 mm of displacement. After the sensor is calibrated, it is bonded with epoxy cement to the relief in the starter notch. These two measurements are typically used to assess the veracity of an analysis of the event. A second strain gage is applied to the specimen about 6 mm above the point of contact at the support pin to ascertain whether the specimen lifts off the support during the fracture event.

A crack gage, manufactured by Hartrun Corporation, is applied to the lateral surface of the specimen to measure the crack growth history. The 50-mm-long crack gage consists of 40 equally spaced, thin metallic rungs 0.25-mm wide and located 1.27 mm on centers, deposited on a thin, flexible, electrically insulated substrate. The gage may be cut to length for different lengths of ligaments. The gage is bonded to the specimen in much the same way that a strain gage is applied. A side groove of the specimen was used as a form to cast a polyurethane piece that conforms to the shape of the side groove. This piece is used to facilitate the placement of the crack gage in the base of the side groove and stability while the epoxy cement cures. Figure 5 shows a specimen with the crack gage installed.

In a test, each rung of the crack gage is wired into a high-speed transient counter, operating at 10 MHz, to monitor the electrical continuity of each rung and to record the time when a rung is broken by the propagating crack tip. A ladder gage with 24 rungs can be applied to the ligament of the bend specimen. Because the high-speed transient counter used in the tests accommodates only 18 channels, not all rungs can be monitored. Typically, each rung except for every 3rd one between the first 5 and last 4 is used in a test. This

arrangement permits the measurement of the crack growth over the entire ligament.

### Test Procedure

The specimen's geometry (length, height, thickness, net thickness in the side groove and initial crack length) and positions of the strain gages and locations of the rungs of crack gage are measured and recorded. The specimen is placed in the supporting fixture and positioned so that the starter notch and the axis of the transmitter bar are properly aligned. Figure 6 shows the crack gage and eddy current proximity gage on the specimen positioned in the supporting fixture. The crack tip strain gage is on the backside and is not visible. A cover plate is placed on the fixture prior to a test to contain the fractured specimen.

The specimen and transmitter bar strain gages are connected to separate high-speed strain conditioners typically used in elastic wave propagation tests. The outputs from these conditioners and from the eddy current proximity (COD) gage are connected to the four channels of a Nicolet digital storage oscilloscope. The sampling interval of the oscilloscope is set at 0.2  $\mu$ s. Electrical connections from each rung of the crack gage are made to the transient counter. The loss of electrical continuity of the first rung of the crack gage, which is positioned slightly ahead of the crack tip, triggers the oscilloscope and defines time zero. The pretrigger is set at  $-300 \mu$ s. A strain gage is also placed on the impact face of the transmitter bar. The output from this gage is connected to a second Nicolet oscilloscope that is slaved with the first one. The impact destroys the electrical continuity of the gage and causes an abrupt change in the output. In this way, the instant of impact is measured relative to crack initiation.

A speed for the striker bar is selected and the gas gun is pressurized according to the calibration for the specific striker bar. All data-recording devices are checked and strain gages zeroed as required. When all systems are ready, the gun is fired. A dedicated timer is used to record the signals from the photodiodes, from which the actual speed of the striker is determined. The oscilloscope data are saved on a floppy diskette and transferred to a spreadsheet at the conclusion of

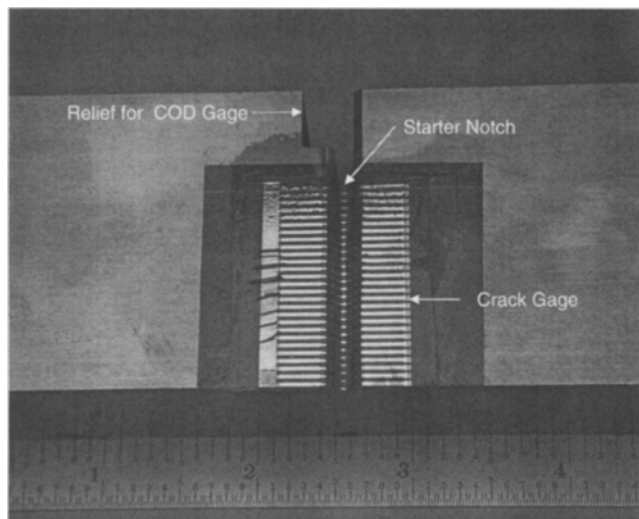


Fig. 5—Close-up view of specimen with crack gage (COD = crack-opening displacement)

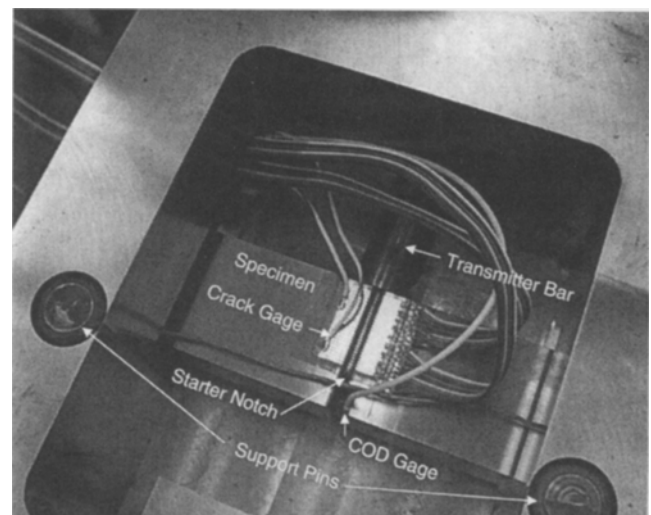


Fig. 6—View of specimen positioned in the specimen holder (COD = crack-opening displacement)

the test. The transient counter times, defining the sequential failure of rungs of the crack gage, are manually recorded and entered onto the same spreadsheet.

### Experimental Results

While a total of six dynamic fracture tests were conducted on AISI 4340 steel specimens for impact speeds ranging from 20.77 m/s to 87.58 m/s, only the results of a single representative test are presented. The results for other tests may be found in Popelar *et al.*<sup>7</sup> The AISI 4340 steel was heat treated to a Rockwell hardness of 48 and had a yield strength of approximately 1500 MPa. The material exhibited quasi-static plane strain fracture toughness of 84.7 MPa-m<sup>1/2</sup> and 80.0 MPa-m<sup>1/2</sup> in two tests using compact tension specimens.

The thickness of the specimen at the base of the side groove is 19.71 mm. The initial crack length including the fatigued precrack was 17.41 mm. For the specific test described here, the striker bar was launched with a speed of 30.47 m/s. Replicate tests demonstrated good repeatability.

Figure 7 shows the measured crack growth history. The crack propagates at nearly a constant speed of 324 m/s, and complete fracture of the specimen takes place approximately 100 μs after crack initiation. Extrapolation of the data to the initial crack length of 17.41 mm indicates that initiation of crack growth occurred at -1.7 μs.

Figure 8 displays the variation of the strain on the surface of the transmitter bar with time. The strain gage is located 63.5 mm from the impact end. The first evidence of straining detected by this gage occurs at -95.2 μs. Because it takes approximately 12.5 μs for a longitudinal wave traveling at 5000 m/s to propagate from the impact end to the strain gage on the transmitter bar, the impact occurred at -107.7 μs. Classical one-dimensional wave theory indicates that the striker bar should produce a strain pulse with an amplitude of 0.3 percent and a duration of approximately 55 μs in the transmitter bar. Radial inertia, neglected in the one-dimensional wave theory, causes the rise of the pulse to occur slightly sooner followed by an overshoot and subsequent oscillatory behavior. When consideration is given to the latter, the first part of the measured amplitude and pulse duration agrees with the simple wave theory estimates. The subsequent signal is complicated by the longitudinal waves reflecting from the impact end of the bar and the interface between the transmitter bar and the fracturing specimen. Interpreting these signals requires a detailed analysis (e.g., see Ref. 7) that is beyond the scope of this paper.

While complete fracture of the specimen occurred at approximately 100 μs, it takes about 37.5 μs (the time for a wave to propagate from the specimen end of the transmitter bar to the strain gage) for this information to be communicated to the strain gage on the transmitter bar. Therefore, the measured strain in the bar for times greater than approximately 138 μs reflects the propagation of a wave trapped within the bar. The period of oscillation is approximately 105 μs and is in good agreement with the round-trip flight time for a longitudinal wave in a 254-mm-long bar.

Figure 9 depicts the strain measured at a site opposite the initial crack tip at a distance of 10 mm. A very rapid rise in the strain occurs as the specimen is loaded through the transmitter bar. Initiation of crack growth can be identified with the first peak of the strain. The peak strain is attained in approximately 40 μs after loading of the crack tip com-

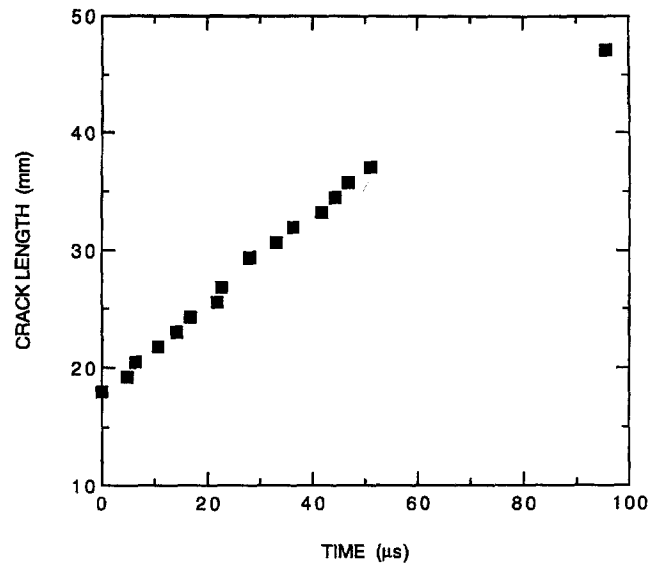


Fig. 7—Measured crack growth history

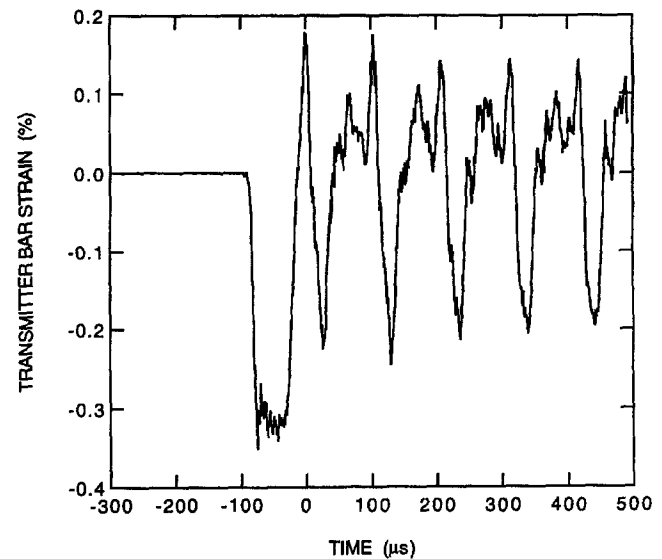


Fig. 8—Measured variation of transmitter bar strain

mences. The material in the neighborhood of the path of the crack quickly unloads and reduces the strain as the crack tip passes. The peak strain in this test was 0.15 percent, which is also indicative of the peak strains recorded in other tests for larger and smaller impact speeds. This suggests that the crack-driving force at crack initiation is independent of the impact speed and is to be expected if the initiation toughness is the same in each test.

The measured COD for this test appears in Fig. 10. The COD commences increasing at approximately -40 μs into the event and attains a value of approximately 0.9 mm at the end of the fracture event at 100 μs.

Figure 11 shows the measured strain at a location 6 mm above the support pin. The signal indicates initially small tensile strains (the spike in the measured signal at -17 μs is thought to be due to electrical noise and not real) followed by much larger compressive strains that ultimately decrease to zero at approximately 119 μs. This time is in excellent agreement with the value obtained when the time of flight

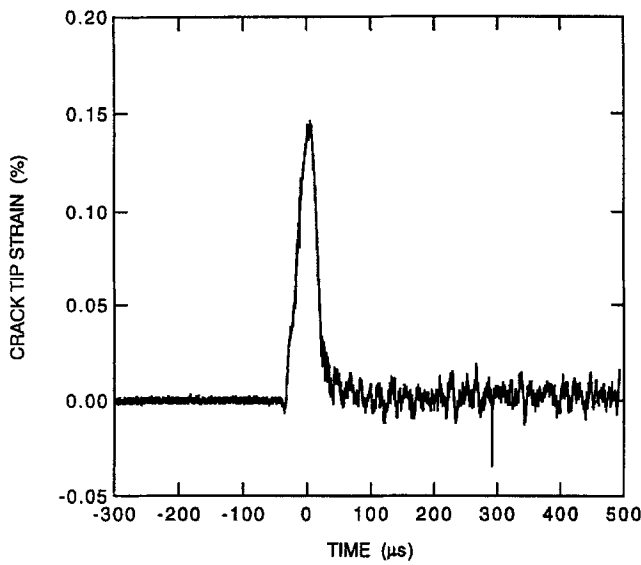


Fig. 9—Measured variation of crack tip strain

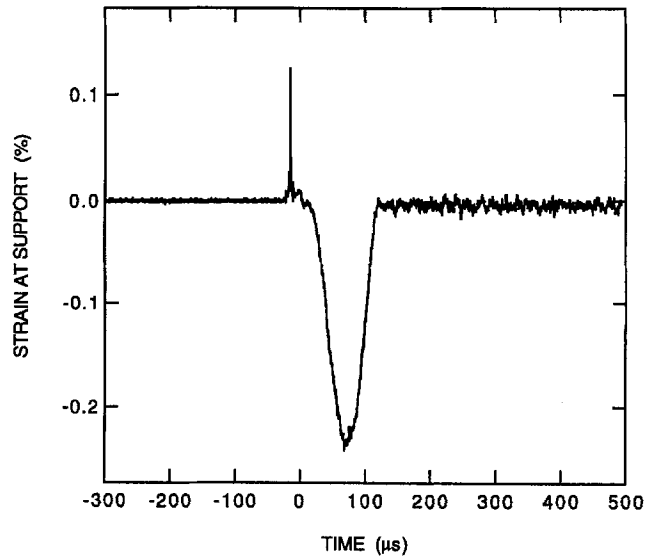


Fig. 11—Measured variation of the strain at the pin support

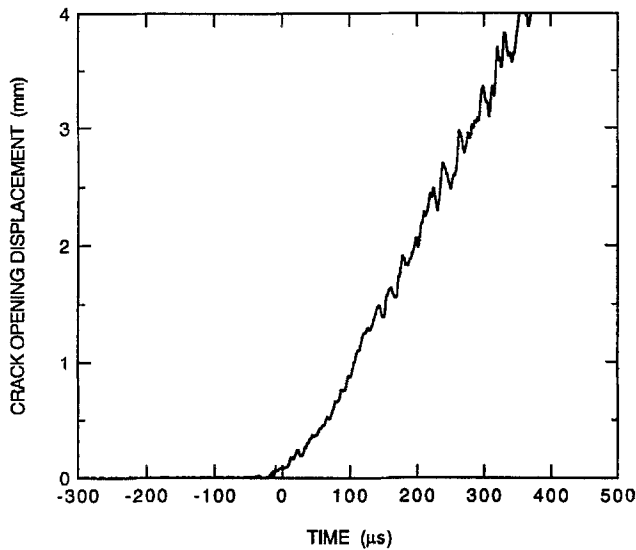


Fig. 10—Measured variation of crack-opening displacement

of approximately 19  $\mu\text{s}$  for a wave to travel from the load point to the support pin is added to the 100  $\mu\text{s}$  fracture event. Except for the initial tensile straining, the results indicate that the specimen remains in contact with the support pin during the fracture event.

Because the initial small tensile strains might be interpreted as indicating that the specimen may have separated from the support pin, a modification was made to the support fixture to prevent the specimen from lifting off the support pins. Further testing with this arrangement produced exactly the same response, including the small tensile strains. Therefore, it was concluded that the specimen does not lose contact with the support. This conclusion was further substantiated by numerical simulations of the tests.<sup>7</sup>

### Fracture Toughness

Guided by the foregoing experimental results, particularly the measured uniform crack growth, a simple quasi-dynamic model is presented for estimating the fracture toughness from dynamic three-point bend tests for materials exhibiting small-

scale yielding. The model is expected to be valid for slightly nonuniform crack growth but not for highly transient crack growth; the latter being beyond the intended purpose of the model. The crack tip opening displacement for plane strain can be approximated as

$$\delta_t = \frac{(1 - \nu^2)K^2}{2E\sigma_o}, \quad (1)$$

where  $\sigma_o$  is the flow stress,  $E$  is the elastic modulus,  $\nu$  is Poisson's ratio and the stress intensity factor  $K$  equals the fracture toughness for the propagating crack. The crack mouth opening displacement may be expressed as

$$\delta_{cmod} = \frac{4aV_1[a/W](1 - \nu^2)K}{\sqrt{\pi a}EF[a/W]}, \quad (2)$$

where  $a$  is the crack length,  $W$  is the height of the specimen and, according to Tada, Paris and Irwin,<sup>8</sup>

$$F[x] = \frac{1.99 - x(1 - x)(2.15 - 3.93x + 2.7x^2)}{\sqrt{\pi(1 + 2x)(1 - x)^{3/2}}} \quad (3)$$

and

$$V_1[x] = 0.76 - 2.28x + 3.87x^2 - 2.04x^3 + 0.66/(1 - x)^2. \quad (4)$$

Assuming that the crack faces remain straight, and using geometric similarity, the COD can be approximated by

$$COD = \frac{(a + c - d)\delta_{cmod}}{a + c}, \quad (5)$$

where

$$c = \frac{a\delta_t}{\delta_{cmod} - \delta_t} \quad (6)$$

and  $d$  is the distance from the edge of the specimen to where the COD is measured, which is 5 mm for the specimens used in this investigation.

In the development of this simple model, the static relation of eq (2) is used in place of the equivalent dynamic relation. The latter is a complicated function of crack speed that reduces to the static relation in the limit as the crack speed tends to zero.<sup>1,9</sup> When the ratio of the crack speed to Rayleigh wave speed (about 3000 m/s for steel) is less than approximately one-third, the static relation can be expected to be an adequate engineering approximation that is consistent with the precision of typical toughness measurements. While the distance  $c$  has been retained for purposes of generality, it could be neglected compared to  $\delta_{cmo}$  for low toughness, high strength materials (e.g., heat-treated AISI 4340 steel), except during the initial stages of crack growth where  $\delta_{cmo}$  may also be small.

For an assumed value of the fracture toughness and the measured crack length, eqs (1) through (6) can be used to calculate the COD, which may be compared with the measured value. Conversely, these equations can be solved iteratively to determine the toughness for measured COD and crack length. Because the measured crack speeds were constant in these tests, the former method for  $E = 200$  GPa,  $\nu = 0.3$ ,  $\sigma_o = 1.51$  GPa and an assumed value of  $K_{ID} = 88$  MPa-m<sup>1/2</sup> is used to compute the COD for the measured crack length history in Fig. 7. Figure 12 compares the predicted COD with the measured values from crack initiation through fracture of this specimen, and the agreement is very good. Similar correspondence was obtained for other tests. In the latter, agreement between predictions and measurements tends to deteriorate somewhat as the crack approaches the impacted face of the specimen. This may be due to plasticity effects that violate the conditions of small-scale yielding. Using only the crack tip singular stress fields and neglecting the effects of side grooves, the computed crack tip strain for  $K = K_{ID} = 88$  MPa-m<sup>1/2</sup> at crack initiation is 0.14 percent and 0.16 percent for plane strain and plane stress, respectively. These values are in good agreement with the measured peak crack tip strain of approximately 0.15 percent at initiation. This close agreement further suggests that the strain gage is within the  $K$ -dominant region and that the side grooves have a negligible influence on the strain at this point (i.e., the effect of the side groove can be neglected in computing this strain). Moreover, this comparison provides an independent validity check of the model. This model offers a simple means for estimating the fracture toughness in lieu of numerical simulation of the test. The crack-driving force of 88 MPa-m<sup>1/2</sup> was attained in approximately 40  $\mu$ s. Therefore, the crack tip loading rate in this test is approximately  $2 \times 10^{-6}$  MPa-m<sup>1/2</sup>-s<sup>-1</sup>. The assumed dynamic fracture toughness  $K_{ID} = 88$  MPa-m<sup>1/2</sup> for the crack speeds ( $\dot{a}$ ) investigated herein is in good agreement with the toughness data determined by Zehnder and Rosakis<sup>3</sup> for AISI 4340 in Fig. 13.

### Conclusions

A dynamic three-point bend test from which the resistance to rapid crack propagation can be evaluated was developed. The magnitude and duration of the loading and, hence, the energy transferred to the specimen are controlled by the speed and length of the striker bar fired by a gas gun. Tests were conducted for AISI 4340 steel. For this material, the rate of crack growth in a test remains virtually constant throughout the propagation event. Therefore, to develop the dependence

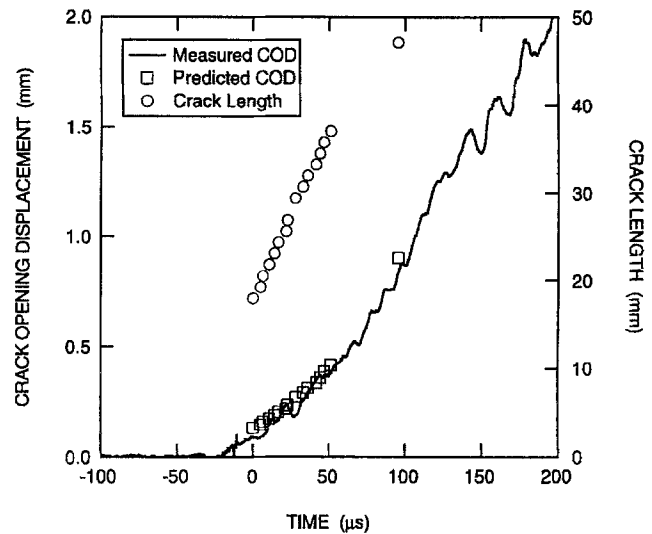


Fig. 12—Comparison of measured and predicted crack-opening displacement (COD)

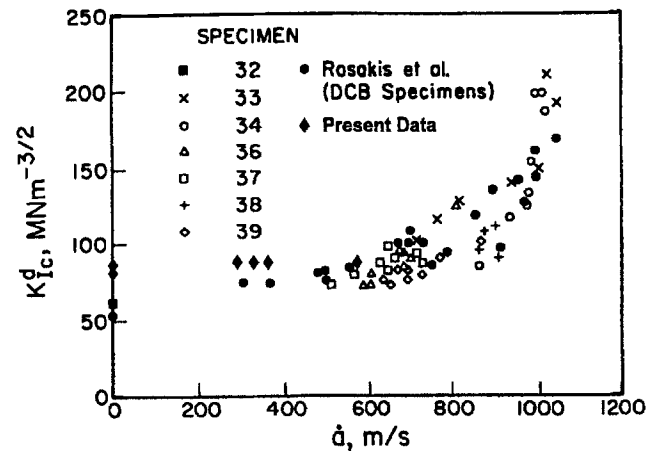


Fig. 13—Comparison of present data with those of Zehnder and Rosakis<sup>3</sup> for AISI 4340 steel (DCB = double cantilever beam)

of the dynamic fracture toughness on the crack growth rate, several tests at different impact speeds are necessary.

Although a gas gun is required, the test is relatively easy to perform. Good repeatability is attainable. The transmitter bar provides an efficient means for transferring the kinetic energy of the striker bar to the specimen without producing penetration and excessive plastic yielding of the specimen that a direct impact by a striker bar can cause. Moreover, the transmitter bar tends to attenuate the highly transient waves that a direct impact of the specimen produces.

A simple engineering model was developed that enables the deduction of the fracture toughness from the COD and crack growth histories measured in the dynamic three-point bend test without the need for a numerical simulation of the test. The method is based on small-scale yielding and, consequently, is limited to high strength, low to moderately tough materials. The model predicted the COD for a propagating crack and crack tip strains at initiation that are in very good agreement with measured values for AISI 4340. While the

fracture toughness was assumed and the COD computed, the measured crack length and COD can be used to determine the fracture toughness as a function of crack speed. Because the crack is found to propagate at a constant speed for a specific test (i.e., striker bar speed), the results are equivalent.

### Acknowledgments

This work was performed under U.S. Air Force Contract No. F08630-96-C-0029. The support of the program manager, Dr. William Cook of the Air Force Research Laboratory, is gratefully acknowledged. The expertise of Art Nichols, who conducted the many experiments, is also acknowledged.

### References

1. Kanninen, M.F. and Popelar, C.H., *Advanced Fracture Mechanics*, Oxford University Press, New York (1985).
2. Couque, H., Leung, C.P., and Hudak, S.J., Jr., "Effect of Planar Size and Dynamic Loading Rate on Initiation and Propagation Toughness of a

Moderate-toughness Steel," *Eng. Fract. Mech.*, **47**, 249–267 (1994).

3. Zehnder, A. and Rosakis, A.J., "Dynamic Fracture Initiation and Propagation in 4340 Steel Under Impact Loading," *Int. J. Fract.*, **43**, 271–285 (1990).

4. van Elst, H.C., "The Evaluation of the Resistance Against Crack Extension by Instrumented High Velocity Impact on 3-Points Bend (Drop Weight Tear Test Like) Specimens in Particular of Linepipe Steel in the Ductile Range Using Gasgun Facilities," *Advances in Fracture Research*, **2**, ed., D. Francois, Pergamon Press, New York, 1059–1072 (1981).

5. Rittel, D., Maigre, H., and Bui, H.D., "A New Method for Dynamic Fracture Toughness Testing," *Scripta Metall. Mat.*, **26**, 1593–1598 (1992).

6. Yokoyama, T., "Determination of Dynamic Fracture-initiation Toughness Using a Novel Impact Bend Test Procedure," *J. Press. Vessel Tech.*, **115**, 389–397 (1993).

7. Popelar, C.H., Walker, J.D., Anderson, C.E., Jr., Johnson, G.R., and Beissel, S.R., "Penetrator Case Fracture Predictive Technology: Volume I—Dynamic Fracture Mechanics Methodology," *Final Report, AFRL-MN-EG-TR-1999-7054*, Air Force Research Laboratory (1999).

8. Tada, H., Paris, P.C., and Irwin, G.R., *The Stress Analysis of Cracks Handbook*, 2nd ed., Paris Production, St. Louis, MO, 2.16–2.17 (1985).

9. Freund, L.B., *Dynamic Fracture Mechanics*, Cambridge University Press, Cambridge (1990).